

InfiCoEvalChain: A Blockchain-Based Decentralized Framework for Collaborative LLM Evaluation

Yifan Yang¹ Jinjia Li² Kunxi Li³ Puhamo Zheng¹ Yuanyi Wang¹ Zheyuan Qu² Yang Yu¹ Jianmin Wu²
Ming Li¹ Hongxia Yang¹

Abstract

The rapid advancement of large language models (LLMs) demands increasingly reliable evaluation, yet current centralized evaluation suffers from opacity, overfitting, and hardware-induced variance. Our empirical analysis reveals an alarming inconsistency in existing evaluations: the standard deviation across ten repeated runs of a single model on HumanEval (1.67) actually exceeds the performance gap among the top-10 models on the official leaderboard (0.91), rendering current rankings statistically precarious. To mitigate these instabilities, we propose a decentralized evaluation framework that enables hardware and parameter diversity through large-scale benchmarking across heterogeneous compute nodes. By leveraging the blockchain-based protocol, the framework incentivizes global contributors to act as independent validators, using a robust reward system to ensure evaluation integrity and discourage dishonest participation. This collective verification transforms evaluation from a “centralized black box” into a “decentralized endorsement” where multi-party consensus and diverse inference environments yield a more stable, representative metric. Experimental results demonstrate that the decentralized evaluation framework reduces the standard deviation across ten runs on the same model to 0.28. This significant improvement over conventional frameworks ensures higher statistical confidence in model rankings. We have completely implemented this platform and will soon release it to the community.

1. Introduction

In recent years, Large Language Models (LLMs) have garnered widespread attention in the field of artificial intel-

¹The Hong Kong Polytechnic University ²InfiX.ai
³Zhejiang University. Correspondence to: Hongxia Yang <hongxia.yang@polyu.edu.hk>, Ming Li <ming.li@polyu.edu.hk>.

Preprint. February 10, 2026.

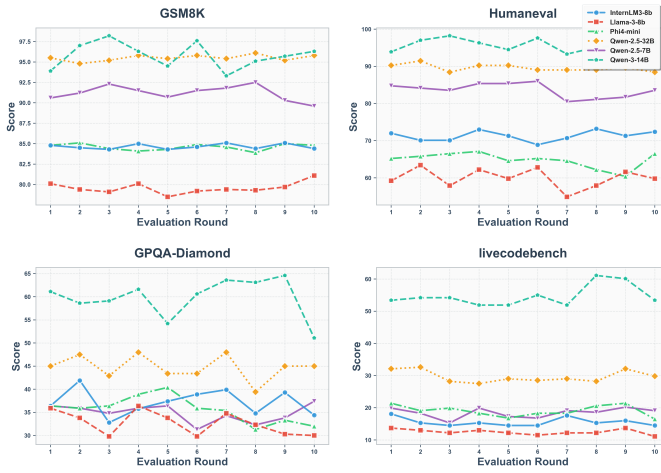


Figure 1. Performance fluctuations of various LLMs Each model was evaluated 10 times on a single computing node with minor variations in inference parameters. The observed variance across all benchmarks highlights the inherent instability of model performance in traditional centralized evaluation settings.

ligence(AI). Their abilities enable AI systems for many downstream tasks to learn, reason, plan and act in the real world in order to help humans (Wang et al., 2024). While these models provide users with more information and improved experiences, they also more directly expose social biases, raising concerns about the safety of LLM (Jung et al., 2025). So far, numerous studies focus on developing different benchmarks to evaluate their capabilities from different aspects. The model runs on these benchmark datasets and generates output results, based on which the evaluation system returns a value representing the model’s capabilities. As is commonly understood, the simplest evaluation benchmark consists of a single dataset on a single task, which is also a common basic evaluation model for natural language processing. To comprehensively evaluate LLMs, multiple datasets are combined and reorganized to form a more universal evaluation benchmark. A valid benchmark means strong results actually reflect the skill being tested. Though these high-quality and reliable LLM benchmarks can effectively guide research, encourage innovation, monitor their advancement, and inform users how to use LLMs for their purpose (Lin et al., 2022; Xu et al., 2025a), they also bring challenges, especially because a few large companies con-

Table 1. Comparison of Standard Deviations of Evaluation Results: “Average” refers to the mean standard deviation of 10 repeated test runs for each model across benchmarks (as shown in Figure 1). “Leaderboard” denotes the standard deviation calculated from the evaluation results of the top 10 models on the respective benchmark.

BENCHMARK	AVERAGE	LEADERBOARD
GSM8K	0.68	0.53
HUMANEVAL	1.67	0.91
GPQA-DIAMOND	2.71	2.28
LIVECODEBENCH	1.68	3.08

trol most of their development, evaluation and application. This concentration of power increases bias in AI systems and reduces the credibility of these models in important decisions (Wang et al., 2025c; Zhou et al., 2025). It leads to the following three concerns:

- **The Statistical Fragility of Generative Evaluation:** The credibility of mainstream LLM benchmarks is undermined by an inherent stochasticity that current evaluation protocols largely ignore. This instability, driven by generative sampling mechanisms and compounded by diverse hardware architectures, renders the common practice of reporting a singular, deterministic score statistically invalid. Our empirical analysis confirms this fragility: as shown in Figure 1, repeated evaluations of state-of-the-art models across benchmarks like GSM8K (Cobbe et al., 2021), HumanEval (Chen et al., 2021), GPQA-Diamond (David et al., 2024), and LiveCodeBench (Jain et al., 2024) reveal significant performance fluctuations. Crucially, our data in Table 1 demonstrates that the standard deviation across ten runs of a single model often matches or exceeds the performance gap among the top-10 models on official leaderboards, suggesting that current rankings may be more a product of environmental noise than actual capability differences (Wang et al., 2025a;b).
- **“Gray Areas” within the evaluation ecosystem:** Common issues include benchmark data leakage into training sets, subtle overfitting to the specific formats and quirks of popular benchmarks, and the exploitation of evaluation methodologies that do not translate to real-world performance. These practices create an opaque and often misleading landscape where headline benchmark scores can diverge dramatically from a model’s true, deployed utility. This erodes trust in published results, stifles meaningful comparison, and potentially misdirects the field’s research priorities.

When the computational and financial costs of model expansion reach unprecedented levels, a rigorous and scientific evaluation framework becomes the primary catalyst for

genuine AI breakthroughs. To address the inherent statistical fragility of generative evaluation, we propose a transition toward a decentralized evaluation ecosystem that leverages a diverse array of evaluators, hardware architectures, and inference configurations for every single model assessment. By aggregating results across a broad spectrum of distributed configurations, we can statistically neutralize the stochastic noise inherent in generative sampling. Furthermore, this approach invites the global research community to provide decentralized endorsements, creating a collective defense against the “gray areas” of data leakage and format overfitting that currently plague the field. However, the inclusion of a distributed network of evaluators necessitates a robust mechanism to guarantee procedural transparency and fairness (Chong et al., 2025). A reliable system must ensure that all participants reach a verifiable consensus on evaluation results while being equitably incentivized for their contributions (Wang et al., 2025c). Blockchain technology provides the essential infrastructure for this vision. By utilizing its decentralized, tamper-resistant ledger, we can ensure that every evaluation run is transparently recorded and audited. This integration not only prevents unauthorized data manipulation but also establishes a trustless framework for reward distribution (Khaled et al., 2019), ultimately paving the way for a more resilient and credible generation of AI benchmarks.

In this paper, our primary objective is to design, implement, and validate a decentralized evaluation framework for generative models, which we call **CoEvalChain** (A Collaborative Evaluation Blockchain). This framework aims to establish a public infrastructure for assessment, with its core design driven by two key imperatives: First, to mitigate the impact of inherent model stochasticity and overfitting on evaluation confidence, we propose a decentralized evaluation paradigm. By introducing a broader spectrum of evaluators, diverse computational resources, and varied inference configurations, we aim to significantly enhance statistical confidence and strengthen the guiding significance of evaluation for model optimization. Second, to ensure the transparency and fairness of this decentralized process, we construct a blockchain as the foundational substrate of the framework. This mechanism not only guarantees the immutable recording of protocols and results but also incorporates a reward system to incentivize broad user participation, thereby establishing a trustworthy and collaborative ecosystem. Our contributions and findings are summarized as follows:

- To the best of our knowledge, we are the first to propose and formally define a decentralized mechanism with blockchain as foundation for generative model evaluation. The blockchain-based architecture ensures the transparency and impartiality of the entire evaluation process, while ensuring the incentive distribution is statistically consistent with the underlying performance

evaluation.

- By evaluating a diverse spectrum of models across a comprehensive suite of benchmarks covering mathematics, coding, and general knowledge, we demonstrate that our decentralized framework effectively mitigates generative stochasticity and hardware-induced noise, delivering significantly more stable and repeatable performance trajectories than traditional centralized methods.
- We successfully implement a functional prototype—a fully operational platform built on the blockchain foundation. And we will release it to the community soon.

2. Method

2.1. Framework of CoEvalChain

As illustrated in Figure 2, CoEvalChain is structured into two synergistic layers designed to bridge community collaboration with decentralized trust. The upper collaborative layer (left) aggregates heterogeneous computing resources from a diverse spectrum of researchers, ranging from individual researchers to institutions, so as to connect them to jointly conduct and endorse large-scale evaluations. Underpinning this is the blockchain-based foundational layer (right), which utilizes a peer-to-peer network to strictly enforce transparency and fairness throughout the evaluation lifecycle. By integrating a consensus protocol with a stable incentivization and punishment mechanism, this foundation ensures the integrity of results and sustains a robust, trust-free ecosystem.

2.2. Rethink the Stochasticity of Generative Model

First of all, our primary objective is to mitigate the inherent stochasticity in LLM outputs, then it is essential to establish a robust evaluation mechanism grounded in statistical and probability theory.

Formally, for a model with a vocabulary size of T and a target sequence length of L , the space of all possible token sequences \mathcal{Y} is of size $|\mathcal{Y}| = T^L$. While the model's training on vast corpora helps it to learn the statistical regularities and co-occurrence patterns of language, the set of plausible responses for a given input prompt still remains exceedingly large and diverse. To analyze this property rigorously, the following section establishes a probabilistic framework to quantify the model's generative uncertainty.

For a given model $Y = f(X)$, we define the expected output for a specific input x_i as $E(f(x_i)) = \hat{y}_i$. Note that this represents the ideal expected output of the model, not the target output.

Therefore, aligning with the prevalent use of cross-entropy optimization in LLMs, the discrepancy between the model's

prediction $y_i = f(x_i)$ and its expected output \hat{y}_i (as defined previously) can be quantified using the binary cross-entropy loss:

$$\ell = -(\hat{y}_i \log(y_i) + (1 - \hat{y}_i) \log(1 - y_i)). \quad (1)$$

Building upon the Eq.(1), we now consider the asymptotic behavior when the model is evaluated at scale. As the number of participants in the benchmark increases, the distribution of possible outputs becomes sufficiently diverse, then the expected discrepancy over the entire benchmark will converge to zero:

$$\lim_{n \rightarrow \infty} \mathbb{E}[\ell] = \lim_{n \rightarrow \infty} \frac{1}{n} \sum_{i=1}^n \ell_i = 0. \quad (2)$$

So by applying a conservative form of the Central Limit Theorem (C.L.T.) on the binary-classification task, a lower bound for the required number of participants n can be derived as

$$n \geq \frac{(1 - 0)^2 \ln\left(\frac{2}{\delta}\right)}{2\varepsilon^2}. \quad (3)$$

Here, ε denotes the margin of error, and $1 - \delta$ represents the confidence level of the estimation.

As an example of applying the derived lower bound, we can calculate the required number of participants n under the confidence level of 80%, with a fixed margin of error $\varepsilon = 0.04$. Suppose we substitute $\delta = 0.2$ and $\varepsilon = 0.04$ into the Eq.(3), we obtain:

$$n \geq \frac{\ln\left(\frac{2}{0.2}\right)}{2 \times (0.04)^2} \approx 28. \quad (4)$$

This implies that, even for a binary classification task, in order to obtain an evaluation conclusion with a confidence level exceeding 80%, it requires more than 20 repeated trials.

Based on the derivation, achieving a high-confidence evaluation necessitates a significant increase in the number of independent observations n . In practical decentralized scenarios, this requirement translates to the imperative of introducing environmental diversity into the evaluation process. Specifically, our framework orchestrates repeated evaluations of the same task across a multi-dimensional configuration space, encompassing varied GPUs, diverse inference configurations, and expanded test data permutations.

Drawing on the statistical analysis proposed by [Miller \(2024\)](#), we further operationalize the measurement of evaluation stability by incorporating standard errors (SE) and 95% confidence interval (CI) as our primary reliability metrics.

We define the scoring metric for a given benchmark as $S = f(Y)$. Consequently, the score for each individual

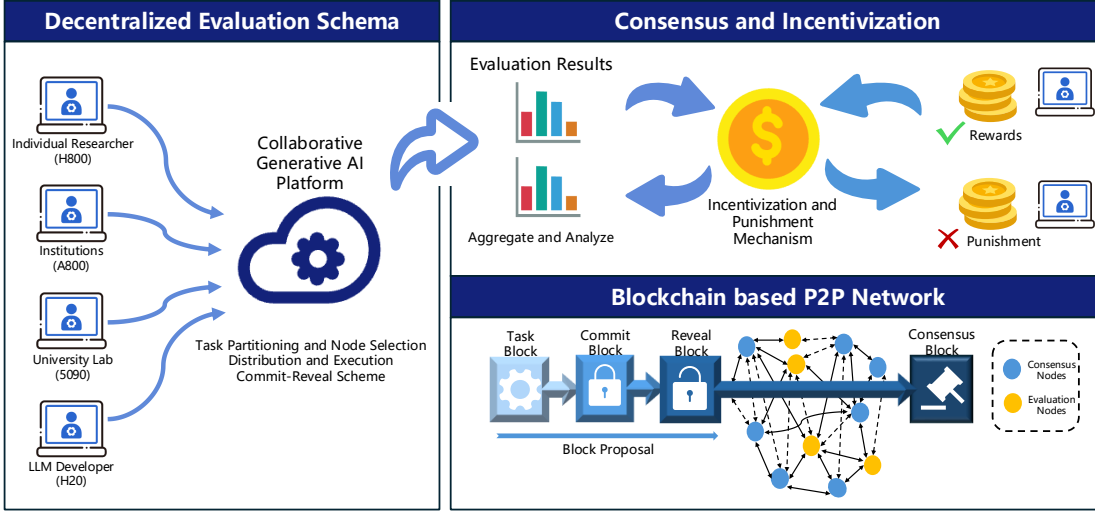


Figure 2. Overview of the CoEvalChain. The framework coordinates heterogeneous computing nodes for collaborative AI tasks (left). An algorithmic incentive mechanism distributes rewards or penalties based on evaluation metrics (top right), while a blockchain-based P2P network ensures integrity through a multi-stage consensus protocol (bottom right).

evaluation instance y_i is expressed as $s_i = f(y_i)$. Let $\bar{s} = \frac{1}{n} \sum_i s_i$ represent the average of the observed scores, based on these individual observations, the standard error of the mean score \bar{s} can be estimated as:

$$SE_{C.L.T.} = \sqrt{\left(\frac{1}{n-1} \sum_{i=1}^n (s_i - \bar{s})^2 \right) / n}. \quad (5)$$

And 95% confidence interval can be computed from:

$$CI_{95\%} = \bar{s} \pm 1.96 \times SE_{C.L.T.}. \quad (6)$$

We further connect these uncertainty estimates with (i) the variance decomposition across heterogeneous configurations and (ii) the required number of independent runs to make leaderboard gaps statistically distinguishable in Appendix C.

2.3. Consensus based on Blockchain

While increasing the diversity of environments and the number of participants n provides the statistical foundation for high-confidence results, it simultaneously necessitates a robust governance framework to ensure evaluation process integrity and facilitate multi-party consensus within a decentralized collective.

So, we establish a multi-layered consensus mechanism starting with a *token-based staking requirement*. Access to evaluation tasks is strictly gated, nodes must stake tokens to participate. This economic barrier serves as a Sybil-resistance mechanism, ensuring that evaluators have “skin in the game”

and aligning their financial interests with the honest execution of tasks.

Considering the inherent stochasticity in LLM benchmarks and the risk of adversarial behavior, we design our consensus logic based on *Schelling Point (Focal Point) game theory* (Schelling, 1980). The evaluation process is modeled as a coordination game where, in the absence of communication, rational nodes maximize their rewards by converging on the “truth” as the natural focal point.

The selection of a Schelling Point in our scenario is predicated on the expectation that other evaluation results will also converge on a specific score. Given a set of available evaluation result S for all participants, the focal point $s^* \in \prod S$ is achieved when salience is maximized:

$$\text{Schelling Point } s^* = \arg \max_{s \in S} P(s), \quad (7)$$

where $P(s)$ represents the probability that evaluation result s is perceived as “unique” or “salient” by the collective.

Critically, to enforce the independence required for this game-theoretic equilibrium and to prevent “free-riding” where nodes merely copy others’ results, we tailored a cryptographic *two-phase Commit-Reveal scheme*:

- **Commit Phase:** Upon evaluating the model, evaluator i generates a score s_i and a random cryptographic salt r_i . Instead of broadcasting the score directly, the evaluator computes a commitment hash $C_i = \text{Hash}(s_i \parallel r_i)$ and broadcasts C_i to the ledger. It ensures the score s_i remains secret, preventing information leakage while locking the evaluator’s decision.

- **Reveal Phase:** Once the commitment window closes, the protocol enters into the reveal phase. Evaluators broadcast their original parameters (s_i, r_i) , then the smart contract validates that $\text{Hash}(s_i \parallel r_i)$ matches the previously recorded C_i . After that, s_i can be accepted in the final candidate set for consensus calculation.

2.4. Incentivization Mechanism

Building upon the integration of diverse evaluation environments and multiple researchers, it is imperative to ensure that the decomposition of evaluation tasks remains both systematic and logical. To this end, we introduce two foundational modules: one dedicated to the strategic partitioning of benchmark datasets, and another for the rigorous screening of on-chain participants based on their historical contribution records and evaluation quality (the formal specifications for these stages are detailed in Appendix A and Appendix B). Furthermore, to sustain long-term participant engagement and align the economic interests of evaluators with the accurate execution of tasks, we implement the following incentivization distribution mechanism.

To ensure the reliability of the evaluation process and mitigate the influence of outliers, we design a proximity-based incentive strategy. Unlike mean-based approaches, which are susceptible to skewing by extreme values, our mechanism leverages the median as a robust reference point. The core ideas include calculating the median of the batch evaluation results and assigning rewards proportional to the proximity of an evaluator’s submission to this median.

Let $\mathcal{S} = \{S_1, S_2, \dots, S_n\}$ denote the set of evaluation results submitted by n evaluators. The median of the above submissions \mathcal{S} is defined as M : $M = \text{median}(s_1, \dots, s_n)$

For each evaluator i , we derive an individual score weight w_i using a Gaussian decay function, ensuring that the influence of a submission decreases non-linearly as its deviation from the median increases:

$$w_i = \exp\left(-\frac{(s_i - M)^2}{2\sigma^2}\right), \quad (8)$$

where σ is a tuning parameter derived from the Median Absolute Deviation (MAD) to ensure robustness against adversarial behavior. We calculate $\text{MAD} = \text{median}(|s_i - M|)$ and set $\sigma = k \cdot \text{MAD}$, where $k \in [1, 1.5]$ is a hyper-parameter controlling the decay rate.

To maintain the stability of the on-chain economy and prevent excessive token inflation, we implement a fixed-pool reward distribution. For each evaluation task, a constant total reward R_{total} (currently set to 100 tokens) is allocated. The final reward R_i awarded to the i -th evaluator is calculated as a fraction of this pool, proportional to their

normalized weight:

$$R_i = R_{total} \cdot \frac{w_i}{\sum_{j=1}^n w_j}. \quad (9)$$

This weight-based normalization ensures that the total token issuance remains invariant to the number of participants n , effectively anchoring the token value while rewarding evaluators based on the statistical consensus of the batch.

3. Experiment

3.1. Experimental Setup

Benchmark and Model Selection: To ensure a holistic assessment of LLM capabilities, we curated a benchmark suite covering three core domains: mathematics, coding, and general knowledge. A critical criterion for our selection was data volume; to mitigate the impact of small-sample bias on evaluation accuracy, we excluded sparse datasets in favor of those with substantial test cases. Specifically, all selected benchmarks—(GSM8K (Cobbe et al., 2021), HumanEval (Chen et al., 2021), LiveCodeBench (Jain et al., 2024), GPQA-Diamond (David et al., 2024), and MMLU (Hendrycks et al., 2020)) contain at least hundreds of instances, with MMLU and GSM8K exceeding a thousand. Regarding the models under test, our evaluation spans a diverse spectrum of mainstream open-source families, including Qwen-2.5/3, Llama-3, Phi-4, and InternLM-3. Furthermore, we extend this scope to include ultra-large-scale models such as DeepSeek-V3.2 and Gemini-2.5-Flash to validate the framework’s scalability and stability across varying parameter magnitudes.

Multi-Dimensional Evaluation Configuration: The evaluation is structured across three distinct configuration dimensions to simulate the complexity of decentralized environments. First, at the hardware level, we utilize a heterogeneous mix of NVIDIA H800, A800, and RTX 5090 GPUs to capture performance variations across different computing resources. Second, regarding inference parameters, we systematically vary Temperature, Top-P, Top-K, and Repetition-Penalty to analyze generative stochasticity. Third, for data distribution, full datasets are partitioned into specific subsets based on our proposed algorithm. Ultimately, each evaluation task is executed under ten distinct configuration profiles, which collectively constitute a single comprehensive evaluation round, ensuring that the final performance estimate is robust against environmental and parametric noise.

3.2. Analysis

As shown in Figure 3 and Table 2, decentralized evaluation consistently yields superior stability across all model scales, including DeepSeek-V3.2 and Gemini-2.5-Flash. The line charts illustrate a marked reduction in score volatility, re-

Table 2. Statistical Comparison of Decentralized and Centralized Evaluation Paradigms. This table presents the mean scores, standard deviations (std), and 95% confidence interval (CI) for five LLMs across five diverse benchmarks, comparing the decentralized framework against traditional centralized baselines. The lower standard deviations and narrower confidence intervals in the decentralized setting demonstrates that the decentralized evaluation successfully achieves superior statistical precision and evaluation stability. All detailed data is provided in Appendix D

Model	Evaluation Method	GSM8K			Livecodebench			Humaneval			GPQA-Diamond			MMLU		
		mean	std	95% CI	mean	std	95% CI	mean	std	95% CI	mean	std	95% CI	mean	std	95% CI
Qwen-2.5-7B	Decentralized	91.09	0.13	± 0.090	18.99	0.37	± 0.261	84.06	0.30	± 0.216	34.60	0.88	± 0.627	72.46	0.10	± 0.077
	Centralized	91.2	0.91	± 0.650	18.45	1.57	± 1.12	83.60	1.92	± 1.371	34.85	1.94	± 1.391	74.48	0.16	± 0.116
InternLM-3-8B	Decentralized	85.51	0.17	± 0.125	16.53	0.20	± 0.144	75.16	0.39	± 0.279	36.78	0.51	± 0.367	71.90	0.45	± 0.321
	Centralized	84.65	0.32	± 0.232	15.56	1.31	± 0.939	71.30	1.38	± 0.999	37.16	2.83	± 2.027	71.87	0.41	± 0.296
Llama-3-8B	Decentralized	79.68	0.18	± 0.133	12.75	0.20	± 0.142	60.89	0.49	± 0.352	33.31	1.27	± 0.909	63.44	0.14	± 0.100
	Centralized	79.59	0.71	± 0.509	12.48	0.86	± 0.617	59.95	2.63	± 1.882	32.69	2.60	± 1.859	63.78	0.15	± 0.111
Phi-4-Mini	Decentralized	84.48	0.66	± 0.473	17.10	0.28	± 0.197	68.91	0.95	± 0.680	34.28	1.36	± 0.976	68.50	0.32	± 0.227
	Centralized	84.59	0.40	± 0.287	19.06	1.75	± 1.249	64.81	2.07	± 1.481	35.59	2.83	± 2.026	71.59	0.32	± 0.227
Qwen-3-14B	Decentralized	95.88	0.14	± 0.098	43.45	0.48	± 0.341	93.54	0.44	± 0.312	59.38	0.92	± 0.656	82.63	0.17	± 0.125
	Centralized	96.14	0.25	± 0.176	54.71	3.29	± 2.355	95.79	1.60	± 1.143	59.76	4.25	± 3.04	96.14	0.25	± 0.176

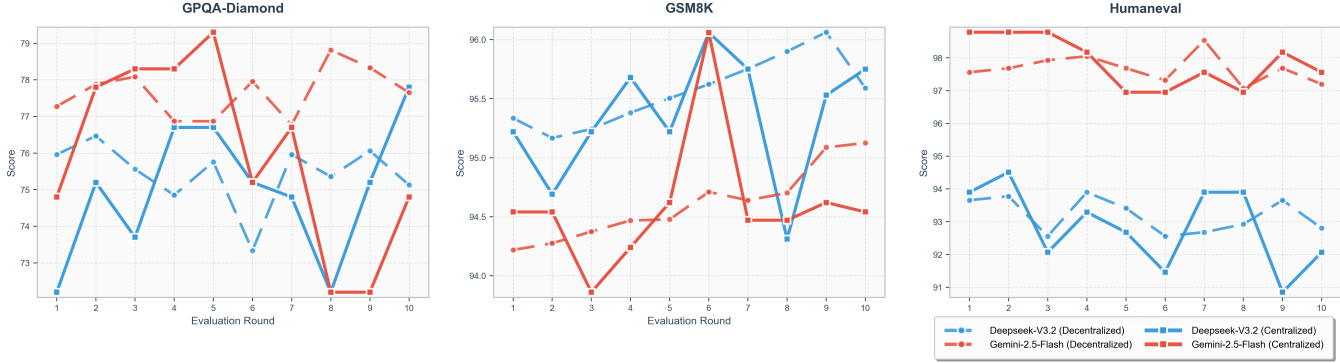


Figure 3. Stability Comparison of Evaluation Paradigms on Large-scale Closed-source Models. Across multiple benchmarks (GPQA-Diamond, GSM8K, and Humaneval), the decentralized evaluation framework (dashed lines) consistently exhibits significantly lower variance compared to the centralized approach (solid lines). This trend holds true even for high-parameter models such as DeepSeek-V3.2 and Gemini-2.5-Flash, demonstrating that decentralization effectively mitigates the inherent stochasticity in large-scale model inference.

placing the erratic fluctuations of centralized testing with smooth, repeatable trajectories. This stabilizing effect is most significant in high-difficulty benchmarks like LiveCodeBench and GPQA-Diamond. For instance, the std for Qwen-3-14B on GPQA-Diamond drops from 4.25 to 0.92. By aggregating across diverse hardware and inference configurations, the decentralized approach effectively neutralizes generative noise, providing a more reliable capability estimate for both small and large-scale models.

Overall Stability Improvements: As detailed in Table 2, decentralized evaluation yields superior stability metrics compared to centralized baselines. For example, Qwen-2.5-7B on the GSM8K benchmark exhibits a dramatic reduction in standard deviation (std), dropping from 0.91 in the centralized setting to 0.13 in the decentralized setting. Similarly, the 95% Confidence Interval (CI) tightens sig-

nificantly from ± 0.650 to ± 0.090 , providing a much more precise estimation of the model’s true capability.

Impact on Difficult Tasks: The stabilizing effect of our framework is most pronounced in “hard” benchmarks (e.g., GPQA-Diamond and LiveCodeBench), where models typically achieve lower mean scores. These tasks possess higher inherent stochasticity: the complexity of the reasoning chains creates more opportunities for divergent generation paths, leading to extreme score volatility in singular environment. For Qwen-3-14B evaluated on GPQA-Diamond (mean score ≈ 59), the centralized evaluation suffers from massive instability (std of 4.25, CI of ± 3.04). The decentralized setup drastically corrects this, reducing the std by over 78% to 0.92.

Analysis Across Model Scales: It is a common heuristic

Table 3. Stability Assessment of Decentralized Evaluation on Large-Scale Models. This table reports the mean, standard deviation (std), and 95% confidence interval (CI) for large-scale models across three benchmarks. The results highlight that the decentralized evaluation framework consistently yields lower standard deviations and narrower confidence intervals compared to centralized baselines.

Model	Evaluation Method	GSM8K			Humaneval			GPQA-Diamond		
		mean	std	95% CI	mean	std	95% CI	mean	std	95% CI
Gemini-2.5-Flash	Decentralized	94.61	0.31	± 0.223	97.66	0.43	± 0.309	77.65	0.69	± 0.494
	Centralized	94.60	0.56	± 0.403	97.86	0.77	± 0.554	75.96	2.53	± 1.809
Deepseek-V3.2	Decentralized	95.56	0.29	± 0.207	93.19	0.54	± 0.385	75.44	0.88	± 0.630
	Centralized	95.34	0.53	± 0.379	92.86	1.22	± 0.874	74.97	1.86	± 1.331

that increased parameter counts correlate with robust and stable performance. We extend the experiment to massive proprietary models. Gemini-2.5-Flash, despite its scale, exhibited a higher *std* of 2.53 on GPQA-Diamond with centralized evaluation, which is comparable to the 8B class. Decentralized evaluation tightened this to 0.69, it means that decentralized evaluation becomes equally, not less important as model scale increases.

3.2.1. INCENTIVIZATION ANALYSIS

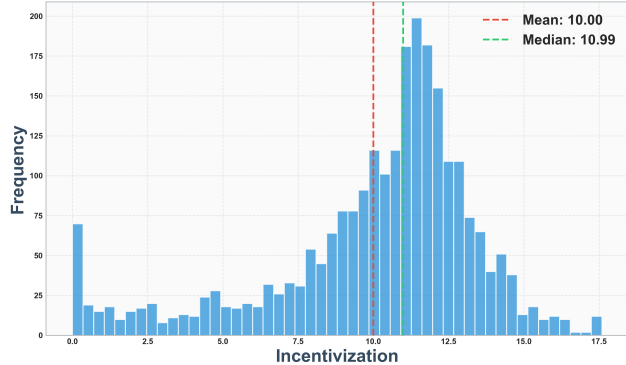


Figure 4. Distribution of Evaluator Incentivization Across the Decentralized Experiment. This histogram illustrates the distribution of incentives allocated to evaluators across all benchmark sessions within our framework. The data exhibits a clear Gaussian-like distribution centered around the collective consensus, demonstrating the consistency and fairness of the incentive mechanism. Notably, the presence of isolated frequency bars near zero represents the effective identification and penalization of outliers—evaluators whose submissions deviated significantly from the robust median baseline.

We apply the proposed incentivization mechanism to calculate rewards for all participating evaluation nodes. As a simulation of a blockchain-based reward system, it provides quantitative insights into the stochastic nature of LLM. Based on the reward distribution illustrated in Figure 4, two key observations can be derived:

- **Community Stability:** The incentivization is determined by the evaluation scores from each node. While the distribution approximates a normal curve centered around the 11.0–11.5 interval (where the peak frequency approaches 200), there is a notable cluster of outliers at the lower bound. Specifically, the reward of a frequency of roughly 70 nodes (approximately 3% of the total population) is observed close to 0, indicating these nodes received minimal rewards due to significant deviation from the consensus. But the vast majority falls within the central range, suggesting the mechanism effectively maintains community stability.

- **Variance in LLM Inference:** Apart from the outlier cluster at zero, the distribution is highly concentrated, with the bulk of the rewards falling between 7.5 and 14.0. This aligns with the general understanding of LLM capabilities: despite the inherent stochasticity of the inference process, the variance remains within a bound.

3.2.2. EFFECT OF TASK PARTITION

To evaluate the effectiveness of our data partitioning strategy, we present a comparative analysis of model performance across different subsets in Table 4. The empirical results demonstrate that our proposed stratification method successfully maintains consistent difficulty levels across partitions.

Table 4. Model Performance Across Stratified Partitions. This table compares Gemini-2.5-Flash and Deepseek-V3.2 performance across GSM8k, Humaneval, and GPQA-Diamond subsets, partitioned via stratified sampling to ensure balanced task complexity. The minimal performance variance observed across all three benchmarks validates the strategy’s effectiveness in achieving uniform difficulty stratification

Benchmark	Gemini-2.5-Flash		Deepseek-V3.2	
	partition-1	partition-2	partition-1	partition-2
GSM8k	94.69	94.52	95.53	95.57
Humaneval	98.29	97.04	95.95	90.44
GPQA-Diamond	76.73	78.57	77.05	73.84

For most benchmarks, both models exhibit remarkable stability across subsets. For example, in the experiment of GSM8K, Gemini-2.5-Flash maintains a performance of 94.69% in partition-1 and 94.52% in partition-2, while Deepseek-V3.2 shows an even tighter margin with 95.53% and 95.57%, respectively. Similar consistency is observed in the GPQA-Diamond benchmark, where both models demonstrate minimal fluctuations across different partitions. This minimal variance confirms that our algorithm effectively distinguishes mathematical logic and specialized knowledge tasks with high uniformity.

While the partitions are generally balanced, we observe a

more noticeable performance delta in the HumanEval benchmark, particularly for Deepseek-V3.2 (95.95% in partition-1 vs. 90.44% in partition-2). Interestingly, while GPQA-Diamond remains stable despite its high difficulty, the variance in HumanEval likely stems from the high sensitivity of coding tasks to specific logic patterns. In these cases, even minor differences in sample composition or the inherent complexity of a few edge-case programming problems can lead to more pronounced fluctuations in success rates compared to other tasks.

4. Related work

4.1. Blockchain used with Large Language Models

To date, the majority of machine learning and deep learning methods of AI rely on a centralized model for training in which a group of servers run a specific model against training and validating datasets, many powerful companies manage the huge volumes of data to make informed decisions (Khaled et al., 2019; Dinh & Thai, 2018). Obviously, the centralized nature of LLMs may lead to an increasing bias in AI systems and reduce the credibility of models. As a decentralized technology, Blockchain has already enabled a wide applications, from cryptocurrencies and digital asset management to accountable data sharing (Shamsi et al., 2022; Xu et al., 2023; Zhang et al., 2023). Considering the centralization poses critical challenges to the continued growth of LLMs, some blockchain-based framework, like LLM-Net(Chong et al., 2025), AIArena(Wang et al., 2025c) and mABC(Zhang et al., 2024), are proposed to ensure sustained knowledge growth, AI democratic development and hallucination mitigation. Additionally, there have been concerns regarding on sorts of LLMs-based applications, such as designing to mine users intent behind DeFi transactions (Mao et al., 2025), and maintaining high standards of smart contract writing practices(Li et al., 2025).

In a nutshell, coupled with the continuous progress, considerable advancements for LLMs have been attained. So, reliable evaluation plays a crucial role in revealing whether a test truly measures what it claims. Yet, centralized issues continue to impede prominent improvements in this field. The blockchain technology with decentralized nature provides novel approaches for resolving these issues. Their combination uncovers substantial opportunities and growth prospects (Gong et al., 2024). How to give a better evaluation is the focus of this paper.

4.2. Evaluation for Large Language Models

With the advancement of LLMs, they have been used across diverse fields, serving as partners to provide intelligence in our daily work and life. Obviously, the AI decision outcomes should be high-quality, safety, and credibility. To

this end, a rich ecosystem of standardized benchmarks has emerged to quantify LLM performance (Feng et al., 2025a; Guo et al., 2025). It raises a fundamental question: What better LLM benchmarks look like. We believe that the following critical points are essential: 1)defining exactly what each benchmark measures: Focused on measuring how models mimic human falsehoods, the expertise benchmarks (Lin et al., 2022; Ji et al., 2023; Mou et al., 2024; Yin et al., 2024) are introduced to demonstrate the challenges toward improved safety alignment. In (Guo et al., 2025), a graduate-level, multi-disciplinary and English-Chinese benchmark is proposed to assess the reasoning capability. BBQ(Parrish et al., 2022) focus on how social biases manifest in model outputs. 2)Strong statistical methods and fair estimates are essential for meaningful tests. Based on mutual information, researchers design GEM, as an evaluation metric to assess generated results without gold standard reference (Xu et al., 2025b), while others construct the frameworks or the dataset drawing on statistical theory to benefit the design of LLMs(Liu et al., 2024; Meister et al., 2025; Miller, 2024; Qian et al., 2026).

Yet, Human evaluation remains the gold standard in LLMs' evaluation. A comparative study of the stochastic process underlying the texts produced by LLMs and human beings is offered (Santis et al., 2024). Aiming to evaluate the alignment with human preferences, the platform(Chiang et al., 2024; Feng et al., 2025b) allow crowdworkers to compare model outputs directly. However, existing research rarely addresses the inherent randomness in LLM inference, which often undermines the reliability of benchmark results. Our work aims to mitigate this stochasticity, ensuring that benchmarks yield more confident evaluations and truly reflect models' actual capabilities.

5. Conclusion

This paper addresses the critical reliability gaps in current centralized LLM evaluation by proposing a decentralized evaluation framework. Our approach leverages blockchain-based protocols and multi-party consensus across heterogeneous compute nodes to validate model performance. Experimental results demonstrate that this collective verification effectively neutralizes generative noise, significantly reducing the evaluation standard deviation from 1.67 to 0.28. While our current implementation focuses on text-based benchmarks, future work will extend this paradigm to multi-modal models. And once the platform is officially released and has accumulated a significant user base, we intend to conduct comprehensive user analysis and surveys to explore economic models and maintain the long-term sustainability of this community. Ultimately, this framework shifts the evaluation landscape from a “centralized black box” to “decentralized endorsement ecosystem”, providing a more stable and representative metric for the AI community.

6. Impact

Elevating Evaluation Reliability: By transitioning from a “centralized black box” to a “decentralized endorsement”, our framework fundamentally addresses the inherent statistical fragility and hardware-induced variance currently plaguing generative AI assessment. We anticipate that the resulting high-confidence leaderboards will provide the global research community with a more stable and representative metric. Such precision is critical for model optimization, as it allows developers to distinguish genuine architectural breakthroughs from mere environmental noise, thereby offering more accurate guidance for iterative model refinement.

Establishing a Blockchain-Based Collaborative Platform for Community Progress: Beyond its technical utility, this framework seeks to cultivate a new community-centric product for the generative AI era. By utilizing a blockchain-based foundational layer, we ensure procedural transparency, immutable recording of results, and an equitable incentive mechanism. This decentralized ecosystem invites global contributors—from individual researchers to large institutions—to participate as independent validators. We believe that this platform will evolve into a robust public infrastructure for model assessment, democratizing the evaluation process and serving as a primary catalyst for sustained, collaborative progress in generative model technology.

References

Chen, M., Tworek, J., Jun, H., Yuan, Q. M., Pinto, H. P., Kaplan, J., Edwards, H., Burda, Y., Joseph, N., Brockman, G., and et al. Evaluating large language models trained on code. *arxiv preprint arxiv:2107.03374*, 2021.

Chiang, W., Zheng, L., Sheng, Y., Nikolas, A., Li, T., Li, D., Zhu, B., Zhang, H., Jordan, M., Gonzalez, J., and et al. Chatbot arena: An open platform for evaluating LLMs by human preference. In *Forty-first International Conference on Machine Learning (ICML 2024)*, Vienna, Austria, 2024.

Chong, Z., Ohsaki, H., and Ng, B. LLM-Net: Democratizing LLMs-as-a-service through blockchain-based expert networks. In *Proceedings of the 2025 14th International Conference on Software and Computer Applications (ICSCA 2025)*, pp. 313–320, Kuala Lumpur, Malaysia, 2025.

Cobbe, K., Kosaraju, V., Bavarian, M., Chen, M., Jun, H., Kaiser, L., Plappert, M., and et al. Training verifiers to solve math word problems. *arxiv preprint arxiv:2110.14168*, 2021.

David, R., Hou, B. L., Stickland, A. C., Petty, J., Pang, R. Y., Dirani, J., Michael, J., and Bowman, S. R. Gpqa: A graduate-level google-proof q&a benchmark. In *First Conference on Language Modeling (COLM 2024)*, Philadelphia, Pennsylvania, 2024.

Dinh, T. and Thai, M. AI and blockchain: A disruptive integration. *Computer*, 51(9):48–53, 2018.

Feng, K., Ding, K., Tan, H., Ma, K., Wang, Z., Guo, S., Cheng, Y., Sun, G., Zheng, G., Zhang, Q., and et al. Sample-efficient human evaluation of large language models via maximum discrepancy competition. In *Proceedings of the 63rd Annual Meeting of the Association for Computational Linguistics (ACL 2025)*, pp. 10913–10947, Vienna, Austria, 2025a.

Feng, K., Ding, K., Tan, H., Ma, K., Wang, Z., Guo, S., Cheng, Y., Sun, G., Zheng, G., Zhang, Q., and et al. Sample-efficient human evaluation of large language models via maximum discrepancy competition. In *Proceedings of the 63rd Annual Meeting of the Association for Computational Linguistics (ACL 2025)*, pp. 10913–10947, Vienna, Austria, 2025b.

Gong, J., Yan, P., Zhang, Y., An, H., and Liu, L. Blockchain meets LLMs: A living survey on bidirectional integration. *arXiv preprint arXiv:2411.16809*, 2024.

Guo, M., Xu, J., Zhang, Y., Song, J., Peng, H., Deng, Y., Dong, X., Nakayama, K., Geng, Z., Wang, C., and et al. R-bench: Graduate-level multi-disciplinary benchmarks for LLM & MLLM complex reasoning evaluation. In *International Conference on Machine Learning (ICML 2025)*, Vancouver, Canada, 2025.

Hendrycks, D., Burns, C., Basart, S., Zou, A., Mazeika, M., Song, D., and Steinhardt, J. Measuring massive multitask language understanding. *arXiv preprint arXiv:2009.03300*, 2020.

Jain, N., Han, K., Gu, A., Li, W. D., Yan, F. J., Zhang, T. J., Wang, S. D., Solar-Lezama, A., Sen, K., and Stoica, I. Livecodebench: Holistic and contamination free evaluation of large language models for code. *arXiv preprint arXiv:2403.07974*, 2024.

Ji, J., Liu, M., Dai, J., Pan, X., Zhang, C., Bian, C., Chen, B., Sun, R., Wang, Y., and Yang, Y. Beavertails: Towards improved safety alignment of LLM via a human-preference dataset. *Advances in Neural Information Processing Systems (Neurips 2023)*, 36:24678–24704, 2023.

Jung, D., Lee, S., Moon, H., Park, C., and Lim, H. FLEX: A benchmark for evaluating robustness of fairness in large language models. In *The Nations of the Americas Chapter of the Association for Computational Linguistics (NAACL 2025)*, pp. 3606–3620, Albuquerque, New Mexico, 2025.

Khaled, S., Rehman, R., Nishara, N., and Ala, A. Blockchain for AI: Review and open research challenges. *IEEE access*, 7:10127–10149, 2019.

Li, Z., Li, X., Li, W., and Wang, X. SCALM: Detecting bad practices in smart contracts through LLMs. In *Proceedings of the AAAI Conference on Artificial Intelligence(AAAI 2025)*, volume 39, pp. 470–477, Philadelphia, Pennsylvania, 2025.

Lin, S., Hilton, J., and Evans, O. TruthfulQA: Measuring how models mimic human falsehoods. In *Proceedings of the 60th Annual Meeting of the Association for Computational Linguistics(ACL 2022)*, pp. 3214–3252, Dublin, Ireland, 2022.

Liu, Y., Yang, K., Qi, Z., Liu, X., Yu, Y., and Zhai, C. Bias and volatility: A statistical framework for evaluating large language model’s stereotypes and the associated generation inconsistency. *Advances in Neural Information Processing Systems(Neurips 2024)*, 37:110131–110155, 2024.

Mao, Q., Zhang, Y., Chen, J., Zhou, E., and Yan, J. Know your intent: An autonomous multi-perspective LLM agent framework for defi user transaction intent mining. *arXiv preprint arXiv:2511.15456*, 2025.

Meister, N., Guestrin, C., and Hashimoto, T. Benchmarking distributional alignment of large language models. In *Proceedings of the 2025 Conference of the Nations of the Americas Chapter of the Association for Computational Linguistics(NAACL 2025)*, pp. 24–49, Albuquerque, New Mexico, 2025.

Miller, E. Adding error bars to evals: A statistical approach to language model evaluations. *arxiv preprint arxiv:2411.00640*, 2024.

Mou, Y., Zhang, S., and Ye, W. Sg-bench: Evaluating LLM safety generalization across diverse tasks and prompt types. *Advances in Neural Information Processing Systems(Neurips 2024)*, 37:123032–123054, 2024.

Parrish, A., Chen, A., Nangia, N., Padmakumar, V., Phang, J., Thompson, J., Htut, P., and Bowman, S. BBQ: A hand-built bias benchmark for question answering. In *Findings of the Association for Computational Linguistics(ACL 2022)*, pp. 2086–2105, Dublin, Ireland, 2022.

Qian, Q., Huang, C., Xu, J., Lv, C., Wu, M., Liu, W., Wang, X., Wang, Z., Huang, Z., Tian, M., and et al. Benchmark²: Systematic evaluation of LLM benchmarks. *arXiv preprint arXiv:2601.03986*, 2026.

Santis, E., Martino, A., and Rizzi, A. Human versus machine intelligence: Assessing natural language generation models through complex systems theory. *IEEE transactions on pattern analysis and machine intelligence*, 46(7): 4812–4829, 2024.

Schelling, T. C. *The Strategy of Conflict: with a new Preface by the Author*. Harvard university press, 1980.

Shamsi, K., Victor, F., Kantarcioglu, M., Gel, Y., and Akcora, C. Chartalist: Labeled graph datasets for UTXO and account-based blockchains. *Advances in Neural Information Processing Systems(Neurips 2022)*, 35:34926–34939, 2022.

Wang, J., Chu, G., Wang, J., Sun, H., Qi, Q., Wang, Y., Qi, J., and Liao, J. Logexpert: Log-based recommended resolutions generation using large language model. In *Proceedings of the 2024 ACM/IEEE 44th International Conference on Software Engineering: New Ideas and Emerging Results*, pp. 42–46, 2024.

Wang, Y., Gu, Y., Zhang, Y., Zhou, Q., Yan, Z., Xie, C., Wang, X., Yuan, J., and Yang, H. Model merging scaling laws in large language models. *arXiv preprint arXiv:2509.24244*, 2025a.

Wang, Y., Yan, Z., Zhang, Y., Zhou, Q., Gu, Y., Wu, F., and Yang, H. InfiGFusion: Graph-on-logits distillation via efficient gromov-wasserstein for model fusion. *arXiv preprint arXiv:2505.13893*, 2025b.

Wang, Z., Sun, R., Lui, E., Zhou, T., Wen, Y., and Sun, J. AIArena: A blockchain-based decentralized AI training platform. In *Companion Proceedings of the ACM on Web Conference 2025(WWW 2025)*, pp. 1375–1379, Sydney, Australia, 2025c.

Xu, S., Hilton, J., and Evans, O. Benchmarking LLMs’ judgments with no gold standard. *International Conference on Learning Representations(ICLR 2025)*, 2025a.

Xu, S., Lu, Y., Schoenebeck, G., and Kong, Y. Benchmarking LLMs’ judgments with no gold standard. In *The Thirteenth International Conference on Learning Representations(ICLR 2025)*, Singapore, 2025b.

Xu, Y., Xiao, S., Wang, H., Zhang, C., Ni, Z., Zhao, W., and Wang, G. Redactable blockchain-based secure and accountable data management. *IEEE Transactions on Network and Service Management*, 21(2):1764–1776, 2023.

Yin, D., Qiu, A., Huang, K., Chang, K., and Peng, N. Safe-world: Geo-diverse safety alignment. *Advances in Neural Information Processing Systems(Neurips 2024)*, 37: 128734–128768, 2024.

Zhang, W., Guo, H., Yang, J., Tian, Z., Zhang, Y., Yan, C., Li, Z., Li, T., Shi, X., Zheng, L., and et al. mABC: multi-agent blockchain-inspired collaboration for root cause

analysis in micro-services architecture. In *Findings of the Association for Computational Linguistics: EMNLP 2024*, pp. 4017–4033, Miami, Florida, 2024.

Zhang, Z., Luo, B., Lu, S., and He, B. Live graph lab: Towards open, dynamic and real transaction graphs with NFT. *Advances in Neural Information Processing Systems(Neurips 2023)*, 36:18769–18793, 2023.

Zhou, Q., Zhang, Y., Gu, Y., Wang, Y., Sang, Z., Yan, Z., Li, Z., Zhang, S., Wu, F., and Yang, H. Democratizing AI through model fusion: A comprehensive review and future directions. *Nexus*, 2025.

A. Participant Selection

In the sequel, we detail the proposed mechanism on how to select participant nodes. The process involves two primary steps: assessing user quality and selecting nodes diversely based on Maximal Marginal Relevance (MMR).

To evaluate the quality of candidate nodes, we define a composite quality score that balances nodes' historical reputation with task participation frequency. Let r_i denote the reputation of user i , and t_i represent the number of tasks the user has previously participated in. The quality score q_i is defined as:

$$q_i = \frac{r_i}{1 + \gamma \cdot t_i}, \quad (10)$$

where $\gamma \geq 0$ is a penalty coefficient designed to regulate the influence of high-frequency participants. As γ increases, the penalty for users with a higher frequency on participating in past tasks (t_i) becomes stronger, circumventing the monopolization of tasks by a few active nodes while encouraging broader participation.

To avoid homogeneity within the selected nodes, we incorporate a similarity constraint. The similarity between nodes is computed based on two categories of features: **Explicit Features**: Structured attributes including skill keywords, company affiliation, job position, and educational background; **Implicit Features**: Latent characteristics such as themes and specific areas of expertise.

We proposed a module based on the Maximal Marginal Relevance (MMR) algorithm to construct the final participant list. The module utilizes a greedy strategy, iteratively selecting candidates from the unselected set to add to the selected set S . The selection criterion aims to maximize the marginal relevance, defined by the following scoring function:

$$\text{Score} = \lambda \cdot q_i - (1 - \lambda) \cdot \max_{u_j \in S} \text{Sim}(u_i, u_j), \quad (11)$$

where q_i represents the candidate's original quality score, $\max_{u_j \in S} \text{Sim}(u_i, u_j)$ represents the maximum similarity between the candidate u_i and others already in the selected set S . And λ is a hyper-parameter ($0 \leq \lambda \leq 1$) that controls the trade-off between quality and diversity.

The procedure continues until the required number of k individuals is selected.

B. Task Partitioning

Recognizing that the composition of evaluation data exerts a fundamental influence on the final metrics and consensus, we extend our statistical rigor to the pre-execution phase. This begins with a preliminary node selection process to identify the most suitable evaluators for specific tasks based on their computational capabilities and historical reliability (the detailed selection scheme is provided in Appendix A). Building upon this selection, we further design a task partitioning strategy that accounts for both task difficulty and evaluation redundancy to ensure balanced and credible results.

To ensure the statistical validity of the evaluation and the fairness of the workload distribution across the decentralized network, we propose a *Stratified Redundant Partitioning Algorithm*. Let \mathcal{D} denote the whole benchmark dataset, and \mathcal{V} denote the set of selected qualified evaluators (nodes), and N represent the number of selected evaluators from node selection. The partitioning strategy is designed to generate N subsets $\{\mathcal{S}_1, \mathcal{S}_2, \dots, \mathcal{S}_N\}$ subject to a dynamic workload adaptation following two critical constraints:

1. **Redundancy for Consensus Reliability:** To mitigate the subjectivity of individual evaluations and enable the Schelling Point consensus mechanism, every data sample $d \in \mathcal{D}$ must be evaluated by multiple independent nodes. We introduce a redundancy factor ρ ($\rho \geq 1$), guaranteeing that each data point appears in exactly ρ distinct subsets. This overlap is essential for calculating the consensus score and identifying outlier evaluators.
2. **Stratified Difficulty Sampling:** To prevent bias arising from uneven difficulty distribution (e.g., one evaluator receiving only "easy" questions while another receives "hard" ones), we employ stratified sampling. First the benchmark \mathcal{D} is divided into K parts $\{L_1, L_2, \dots, L_K\}$, in which, each part has the same difficulty level. For any generated subset \mathcal{S}_i , the distribution of difficulty levels must mirror the global distribution of \mathcal{D} . It make every evaluator face a representative and heterogeneous mix of tasks, guaranteeing the fairness of the Proof-of-Work (PoW) contribution.

C. Stochasticity in LLM Inference and Sample Complexity

C.1. Evaluation score as a random variable

For a fixed model and benchmark, a single evaluation run does not yield a deterministic value. Instead, the reported score s should be viewed as a realization of a random variable S , induced by decoding randomness, non-deterministic system execution, and configuration choices like hardware, kernel implementations, and inference parameters. Accordingly, the n runs $\{s_i\}_{i=1}^n$ used in Section 2.2 are i.i.d. samples from S , and the sample mean

$$\bar{s} = \frac{1}{n} \sum_{i=1}^n s_i \quad (12)$$

serves as an estimator of the true expected performance $\mu = \mathbb{E}[S]$. This probabilistic view motivates the uncertainty estimates reported in Section 2.2 via the standard error and confidence intervals.

C.2. Variance decomposition across heterogeneous configurations

Let C denote the random execution configuration, including hardware and system-level settings. By the law of total variance, the overall score variance can be decomposed as

$$\text{Var}(S) = \mathbb{E}_C[\text{Var}(S | C)] + \text{Var}_C(\mathbb{E}[S | C]). \quad (13)$$

The first term $\mathbb{E}_C[\text{Var}(S | C)]$ captures run-to-run stochasticity under a fixed configuration, while the second term $\text{Var}_C(\mathbb{E}[S | C])$ reflects systematic shifts across configurations. By aggregating results across diverse computing nodes and inference configurations, this estimator \bar{s} effectively marginalizes the fluctuations inherent in heterogeneous sources, yielding a more stable average. Under approximate independence, its variance satisfies

$$\text{Var}(\bar{s}) = \frac{\text{Var}(S)}{n}, \quad (14)$$

which directly underlies the standard error estimator. This explains why increasing the number of independent runs, especially across diverse configurations, reduces both stochastic noise and configuration-induced bias.

C.3. Sampling complexity for distinguishing leaderboard gaps

Consider two models A and B evaluated under the same protocol, with true means μ_A, μ_B and $\Delta = \mu_A - \mu_B$. Let \bar{s}_A, \bar{s}_B be their sample means obtained from n independent runs each. By the central limit theorem,

$$\bar{s}_A - \bar{s}_B \approx \mathcal{N}\left(\Delta, \frac{\sigma_A^2}{n} + \frac{\sigma_B^2}{n}\right), \quad (15)$$

where σ_A^2, σ_B^2 are the corresponding score variances. To distinguish the two models at the 95% confidence level, it suffices that

$$1.96 \sqrt{\frac{\sigma_A^2}{n} + \frac{\sigma_B^2}{n}} \leq |\Delta|, \quad (16)$$

which yields the sample complexity requirement

$$n \geq \frac{2 \cdot (1.96)^2 \sigma^2}{\Delta^2}, \quad (17)$$

assuming $\sigma_A \approx \sigma_B = \sigma$. This formulation underscores the high inherent volatility of evaluation results, suggesting that narrow gaps on leaderboards are often statistically insignificant. Consequently, it highlights the imperative for a decentralized evaluation framework to ensure reliability.

C.4. Ranking instability and inversion probability

The same analysis quantifies the probability of ranking inversion. Specifically, the probability that model B appears to outperform A is

$$P(\bar{s}_A \leq \bar{s}_B) = \Phi\left(\frac{-\Delta}{\sqrt{\sigma_A^2/n + \sigma_B^2/n}}\right), \quad (18)$$

where $\Phi(\cdot)$ denotes the standard normal CDF(Cumulative Distribution Function). When the gap Δ is comparable to the standard error, this probability approaches 0.5, indicating intrinsically unstable rankings. By increasing n and covering heterogeneous configurations, InfiCoEvalChain reduces the effective variance and thus substantially lowers the ranking inversion probability, complementing the empirical uncertainty estimates reported in Section 2.2.

D. Detailed Tables

Table 5. Experimental Data Across All Models and Benchmarks This table presents the complete collection of evaluation results comparing decentralized and centralized paradigms. Each decentralized data point is derived from the average of results obtained from ten independent sub-group partitions of a full experiment, providing the foundational dataset for our performance and stability analysis.

Model	GSM8K		Livecodebench		Humaneval		GPQA-Diamond		MMLU	
	Decentralized	Centralized								
Qwen-2.5-7B	91.25	91.2	18.66	19.9	83.78	84.76	34.69	36.4	72.56	74.5
	91.15	91.2	19.73	18.3	83.72	84.15	36.01	35.9	72.54	74.6
	91.01	91.3	18.99	15.3	84.28	83.54	35.00	34.8	72.38	74.5
	90.92	91.5	19.08	19.9	84.33	85.37	34.14	35.9	72.62	74.6
	91.29	91.2	18.57	17.3	83.62	85.37	34.10	36.4	72.60	74.4
	90.95	91.5	18.51	16.8	84.35	85.98	33.97	31.3	72.44	74.2
	91.22	91.6	18.92	19.1	84.11	80.49	36.00	34.3	72.34	74.4
	91.00	91.5	19.15	18.6	83.78	81.1	33.84	32.3	72.43	74.8
	91.08	91.3	19.30	20.2	84.22	81.71	33.45	33.8	72.37	74.4
	91.10	91.2	19.06	19.1	84.43	83.54	34.79	37.4	72.34	74.4
InternLM-3-8B	85.71	84.8	16.36	18.1	75.37	72.0	36.51	36.4	71.61	71.5
	85.44	84.5	16.62	15.3	74.97	70.1	36.93	41.9	71.55	71.8
	85.84	84.3	16.40	14.5	74.44	70.1	36.14	32.8	72.87	72.1
	85.34	85.0	16.55	15.3	75.15	73.0	35.94	35.8	71.34	71.5
	85.44	84.3	16.49	14.5	75.40	71.3	36.84	37.4	71.73	72.1
	85.70	84.6	16.81	14.5	74.96	68.9	36.38	38.9	72.06	71.7
	85.39	85.1	16.60	17.6	74.82	70.7	37.45	39.9	72.28	72.2
	85.35	84.4	16.88	15.3	75.37	73.2	37.10	34.8	71.93	72.7
	85.47	85.1	16.38	16.0	75.87	71.3	37.18	39.3	71.55	71.3
	85.42	84.4	16.25	14.5	75.30	72.4	37.32	34.4	72.10	71.8
Llama-3-8B	79.71	80.1	12.65	13.7	61.16	59.2	31.16	35.9	63.35	64.0
	79.73	79.4	13.17	13.0	60.30	63.4	33.18	33.8	63.28	63.6
	79.94	79.1	12.63	12.2	60.48	57.9	33.94	29.8	63.39	63.9
	79.23	80.1	12.80	13.0	61.22	62.2	32.12	36.4	63.64	63.7
	79.64	78.5	12.66	12.2	60.85	59.8	33.28	33.8	63.36	63.7
	79.70	79.2	12.93	11.5	61.43	62.8	34.49	29.8	63.36	63.9
	79.79	79.4	12.51	12.2	60.66	54.9	34.64	34.8	63.67	63.6
	79.69	79.3	12.54	12.2	60.59	57.9	32.11	32.3	63.59	63.9
	79.58	79.7	12.75	13.7	60.43	61.6	35.15	30.3	63.38	63.6
	79.79	81.1	12.86	11.1	61.81	59.8	33.00	30.0	63.36	63.9
Phi-4-Mini	84.73	84.8	16.48	21.4	68.72	65.2	35.30	36.4	69.36	71.4
	83.36	85.1	16.86	19.1	68.78	65.8	34.85	35.9	68.31	71.7
	85.25	84.4	17.34	19.9	68.05	66.5	33.38	36.4	68.48	71.2
	84.70	84.1	17.26	18.3	70.18	67.1	34.75	38.9	68.34	71.8
	83.84	84.3	17.11	16.8	69.88	64.6	34.24	40.4	68.30	71.6
	84.73	84.9	17.13	18.3	68.00	65.2	33.87	35.9	68.48	71.5
	84.27	84.6	17.37	18.3	69.58	64.6	35.62	35.4	68.52	71.8
	85.12	83.9	16.94	20.6	67.88	62.2	32.57	31.3	68.38	71.0
	83.70	85.0	17.15	21.4	70.12	60.4	36.29	33.3	68.50	71.9
	85.14	84.8	17.36	16.5	67.92	66.5	31.94	32.0	68.30	72.0
Qwen-3-14B	95.87	96.1	43.68	53.4	94.02	93.9	58.94	61.1	82.49	85.2
	95.77	96.4	43.05	54.2	93.51	97.0	60.31	58.6	82.92	84.9
	95.86	96.1	42.76	54.2	93.14	98.2	59.15	59.1	82.67	85.1
	95.77	96.4	43.62	51.9	93.71	96.3	58.50	61.6	82.61	84.8
	95.72	96.1	43.32	51.9	92.96	94.5	58.65	54.2	82.53	84.9
	96.07	96.1	43.95	55.0	94.24	97.6	60.53	60.6	82.53	84.7
	95.77	95.8	42.95	51.9	93.23	93.3	58.68	63.6	82.50	85.3
	96.03	95.7	43.08	61.1	93.32	95.1	58.29	63.1	82.43	85.0
	96.09	96.4	44.05	60.1	94.04	95.7	60.62	64.6	82.94	85.2
	95.84	96.3	44.01	53.4	93.27	96.3	60.16	51.1	82.67	84.8